

Influence of the composition of the BiPO₄–BiVO₄ system on the phase formation, morphology, and properties of nanocrystalline composites obtained under hydrothermal conditions

Olga V. Proskurina^{1,2,a}, Ilke Diana Chetinel^{2,b}, Anna S. Seroglazova^{1,2,c}, Victor V. Gusarov^{1,d}

¹Ioffe Institute, 194021 St. Petersburg, Russia

²St. Petersburg State Institute of Technology, 190013 St. Petersburg, Russia

^aproskurinaov@mail.ru, ^bdiana03ridak@gmail.com, ^cannaseroglazova@yandex.ru,

^dvictor.v.gusarov@gmail.com

Corresponding author: Olga V. Proskurina, proskurinaov@mail.ru

ABSTRACT BiPO₄/BiVO₄ nanocrystalline composites were synthesized under hydrothermal conditions. The influence of the initial composition of the system on the phase state, the size of crystallites, and the morphology of the formed particles was determined. The photocatalytic activity of the nanocomposite was studied using the decomposition of methyl violet as an example.

KEYWORDS hydrothermal synthesis, phase formation, nanocrystals, bismuth orthophosphate, bismuth orthovanadate

ACKNOWLEDGEMENTS X-ray diffraction studies were performed employing the equipment of the Engineering Center of the St. Petersburg State Institute of Technology. The research was supported by the Russian Science Foundation Grant 21-13-00260.

FOR CITATION Proskurina O.V., Chetinel I.D., Seroglazova A.S., Gusarov V.V. Influence of the composition of the BiPO₄–BiVO₄ system on the phase formation, morphology, and properties of nanocrystalline composites obtained under hydrothermal conditions. *Nanosystems: Phys. Chem. Math.*, 2023, **14** (3), 363–371.

1. Introduction

Bismuth vanadate BiVO₄ is known as the following crystalline modifications: monoclinic (with the structure of the mineral *clinobiswanite*), tetragonal (with the structure of the mineral *dreyerite*) and rhombic (with the structure of the mineral *pucherite*). Materials based on BiVO₄ with a monoclinic structure exhibit photocatalytic properties when irradiated with visible light [1–3]. The band gap of monoclinic BiVO₄ phase is about 2.4 eV, and that of the tetragonal phase is 2.9 eV [4]. In addition, monoclinic bismuth vanadate is characterized by low toxicity and a high chemical stability under the influence of radiation [5]. Nevertheless, bismuth vanadate in the monoclinic system has rather low charge transfer rate and surface adsorption [6]. The structure of monoclinic bismuth vanadate is modified using various additives for achieving the maximum efficiency of the photocatalyst, and can interfere with the recombination of the generated electron-hole pairs [7–9]. Compounds containing PO₄³⁻ anions are able to improve photocatalytic properties, despite the fact that there are quite wide band gap. Due to the formation of a heterojunction between semiconductors, electrostatic interactions of phosphate anions with positively charged holes, and to inertness with respect to the resulting free electrons, the improvement of photocatalytic properties occurs.

Bismuth phosphate BiPO₄ has three polymorphic crystal structures such as hexagonal (the mineral *xymengite*) with space group P3₁21 and two monoclinic, one of which is unstable at low temperatures and exists only at high temperatures. The low-temperature modification has the space group P2₁/n [10]. The band gap in a xymengite crystal is ~ 4.6 eV, whereas, in the case of a monoclinic structure, it is about 3.8 eV [11]. The review [12] considers methods for the synthesis of BiPO₄ with emphasis on its crystal microstructure, optical and photocatalytic properties, as well as a way to create composites based on BiPO₄ for improving a photocatalytic activity.

Bismuth vanadate of the monoclinic modification can be obtained by several methods, that differ from each other in sets of precursors, synthesis conditions, and the complexity of its implementation. The phase formation for systems containing bismuth and vanadium oxides always proceeds in several sequential-parallel stages with the formation of intermediate products [13]. Bismuth vanadate with the *clinobiswanite* structure can be obtained by flame pyrolysis [14], a high-temperature heat treatment [15], solution combustion [16, 17], soft chemistry methods [18, 19], including solvothermal [5] and hydrothermal methods [20–23]. In some cases, the product is subjected to additional firing at a high temperature in order to completely remove moisture and improve the properties of the material: increase porosity and crystallinity and increase the charge transfer rate. According to [24], the best photocatalytic properties of BiVO₄ appear when the synthesis is completed by heat treatment of the product for 3 hours at a temperature of 500 °C.

Recently, a large number of works have appeared devoted to the creation of semiconductor materials as photocatalysts with heterojunctions that limit electron-hole recombination. From this point of view, investigations of solid solution open a prospect to control the energy band structure of a semiconductor and, at the same time, to build an efficient interface for photocatalysis.

The preparation of heterostructures in the $\text{BiVO}_4\text{-BiPO}_4$ system and the study of their photocatalytic characteristics were considered to [25], where compounds of the $\text{BiVO}_4/\text{BiPO}_4$ system were obtained by growing bismuth vanadate nanoparticles on the surface of bismuth phosphate. In [26], a hollow $\text{BiVO}_4/\text{BiPO}_4$ nanocomposite has been obtained under hydrothermal conditions, and showed great potential for use as a photocatalyst. To improve the photocatalytic characteristics, more complex doped or ternary composites based on $\text{BiVO}_4/\text{BiPO}_4$ are also considered [8, 9].

It is of interest to determine the mutual influence of BiVO_4 and BiPO_4 on the formation of nanocrystalline materials in the $\text{BiVO}_4\text{-BiPO}_4$ system, the possibility of the formation of solid solutions in the system, and also to study the photocatalytic properties of composites in this system.

2. Experimental

Bismuth nitrate $\text{Bi}(\text{NO}_3)_3 \cdot 5\text{H}_2\text{O}$ (analytical grade) in an amount of 4 mmol was dissolved in 10 ml of 6 M nitric acid HNO_3 (chemically pure) with stirring with a magnetic stirrer (solution "A"). An ammonium metavanadate solution was prepared by dissolving an appropriate amount of NH_4VO_3 (analytical grade) in 40 ml of distilled water (solution "B"). To increase the solubility of the salt, the solution was heated to 70 °C. For the synthesis of samples containing bismuth phosphate, solution "C" was prepared by dissolving an appropriate amount of $(\text{NH}_4)_2\text{HPO}_4$ (chemically pure) in cold distilled water.

Solution B was added dropwise to solution A with continuous stirring, resulting in an orange precipitate. After 10 minutes of vigorous stirring, solution C was also added dropwise to the reaction mixture.

The resulting suspension was stirred for 1 hour. At the same time, a 4 M solution of sodium hydroxide NaOH (analytical grade) was added to maintain pH=1. The reaction mixtures were subjected to hydrothermal treatment at 200 °C and a pressure of ~7 MPa for 4 hours. After 4 hours of isothermal exposure, the autoclave was removed from the furnace and cooled at room temperature. The result of precipitate was washed several times with distilled water until a neutral value pH, centrifuged, and dried at 80 °C for 12 hours for removing of moisture from the sample.

Samples of BiVO_4 , BiPO_4 , and $\text{BiVO}_4/\text{BiPO}_4$ compositions with different molar ratios were synthesized.

Determination of the elemental composition of samples, sizes and shapes of particles was carried out using a scanning electron microscope Tescan Vega 3 SBH (Tescan Orsay Holding, Czech Republic) with an attachment for energy dispersive X-ray spectroscopy Oxford Instruments INCA x-act (Oxford Instruments, Oxford, UK). The size characteristics of particles according to electron microscopy data were analyzed using the ImageJ program.

X-ray diffraction patterns were taken at 25 °C on a Rigaku SmartLab 3 diffractometer (Rigaku Corporation, Japan). Diffractograms were recorded in the Bragg-Brentano geometry in the angle range $2\theta = 10 - 60^\circ$ with a step of 0.01° , a shooting rate of $4^\circ/\text{min}$, and using a $K\beta$ filter ($\text{CuK}\alpha$ is radiation). The phase analysis of the samples was determined using the ICSD PDF-2 database. Full profile phase analysis was performed using the *SmartLab Studio IV* program (Rigaku Corporation, Japan). The average crystallite size was determined from non-overlapping reflections of each phase using the Halder-Wagner method [27]. The instrumental broadening of reflections of the samples was taken into account using a standard, which was a SrTiO_3 single crystal in the form of a polished thin plate.

The photocatalytic activity of the samples was studied in the process of catalytic photodegradation of methyl violet (MV) using xenon lamps to simulate visible light with a power of 100 W with a UV filter $\lambda \geq 420$ nm. The dye oxidation process was carried out in an isolated photochemical reactor [28], which included 50 ml beakers with a reaction solution, a magnetic stirrer, and two xenon lamps.

Before starting photocatalytic experiments, colloidal solutions of the corresponding samples with concentration of 0.045 g/L were preliminarily prepared. Then, 3 ml of a 0.1 g/L methyl violet dye solution and 22 ml of distilled water were added to each of the beakers. Thus prepared reaction solutions were kept in the dark for 15 minutes to achieve adsorption-desorption equilibrium. After this time, the reaction mixture was irradiated with visible light with constant stirring for 60 minutes with sampling of 5 ml every 10 minutes to build kinetic dependences and determine the rate constant of the photocatalytic process. The degree of efficiency of photocatalytic degradation was assessed by changing the concentration of MV using an AvaSpec-ULS2048 spectrometer with an AvaLight-XE light source.

A pseudo first order kinetic model was used to describe dye degradation data by the equation:

$$\ln(C_0/C) = K \cdot \tau,$$

where K is the apparent rate constant of the reaction, C_0 and C are the initial dye concentration after adsorption and the current dye concentration at time τ .

3. Results and discussion

The results of the elemental analysis of the samples are presented in Table 1. The designation of the samples in the work corresponds to their numbering in the table. In all samples, the bismuth content slightly exceeded that specified

for the synthesis. This seems to be related to the measurement error. The content of vanadium in samples turned out to be lower than that specified during synthesis. Probably, at $\text{pH}=1$, a part of vanadium did not crystallize in the form of bismuth orthovanadate, but remained in the hydrothermal solution and was washed out by washing the precipitate.

Diffraction patterns of the obtained samples are shown in Fig. 1. Sample 1 after hydrothermal treatment consists of the BiVO_4 monoclinic phase with the clinobiswanite structure (PDF #00-014-0688). Sample 5 is monoclinic BiPO_4 (PDF #00-015-0767). All samples containing both vanadium and phosphorus are two-phase, containing a BiVO_4 monoclinic phase and a BiPO_4 monoclinic phase. Since the content of vanadium in all samples turned out to be lower than that specified for synthesis, the reflections of the phase of monoclinic BiVO_4 are weakly expressed in diffraction patterns of the samples containing vanadium and phosphorus. Analysis of diffraction patterns of the samples shows that monoclinic modifications of vanadate and bismuth phosphate can be obtained by the hydrothermal method under these conditions (4 hours, $200\text{ }^\circ\text{C}$, 7 MPa) (Fig. 1). Data on the phase ratio in the samples were determined using the Rietveld method and are presented in Table 1.

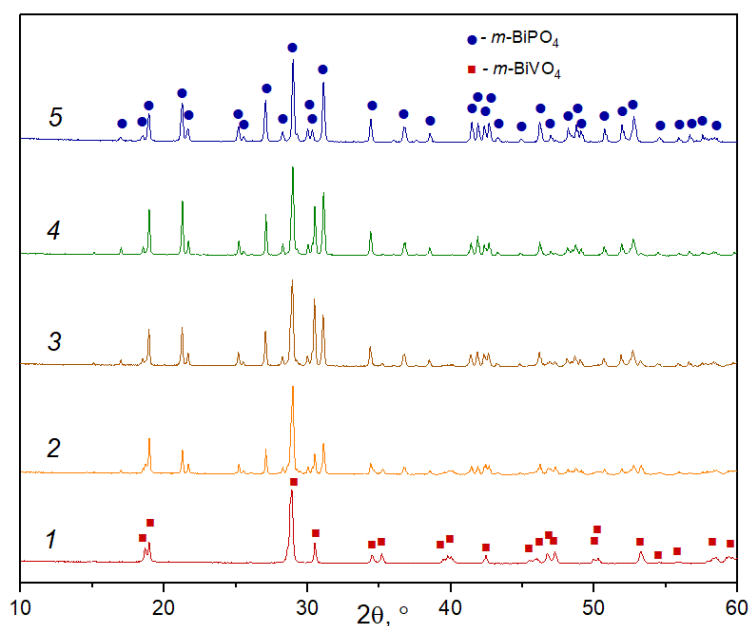


FIG. 1. X-ray diffraction patterns of samples

TABLE 1. Composition of samples

Designation of samples	Composition by synthesis	Composition by analysis (EDX)	Phase composition $m\text{-BiVO}_4 : m\text{-BiPO}_4$ (XRD)
1	BiVO_4	BiVO_4	100 : 0
2	$\text{BiV}_{0.67}\text{P}_{0.33}\text{O}_4$	$\text{BiV}_{0.40}\text{P}_{0.60}\text{O}_4$	41.2 : 58.8
3	$\text{BiV}_{0.50}\text{P}_{0.50}\text{O}_4$	$\text{BiV}_{0.16}\text{P}_{0.84}\text{O}_4$	25.2 : 74.8
4	$\text{BiV}_{0.33}\text{P}_{0.67}\text{O}_4$	$\text{BiV}_{0.12}\text{P}_{0.88}\text{O}_4$	7.3 : 92.7
5	BiPO_4	BiPO_4	0 : 100

The comparison of the data of elemental analysis and X-ray phase analysis showed that for sample 2, the elemental composition coincided with the phase composition of compound according to the analysis almost. For samples 3 and 4, it's shown that there is a decrease and an increase in the proportion of bismuth phosphate compared to elemental analysis, respectively. Further in the work, the composition of the samples will be given according to the data of X-ray phase analysis.

The dependence of the unit cell parameters of both phases on the content of BiPO_4 in the samples allows us to conclude that there is a limited region of the solid solution based on the phase of monoclinic bismuth orthophosphate $\text{BiP}_{1-x}\text{V}_x\text{O}_4$. The unit cell parameters of monoclinic bismuth orthovanadate do not change within the error, which indicates the absence or extremely low solubility of BiPO_4 in the phase based on BiVO_4 . As an example, Fig. 2 shows the dependence of the parameter a of monoclinic phases based on BiPO_4 and BiVO_4 on the $\text{BiVO}_4 : \text{BiPO}_4$ ratio.

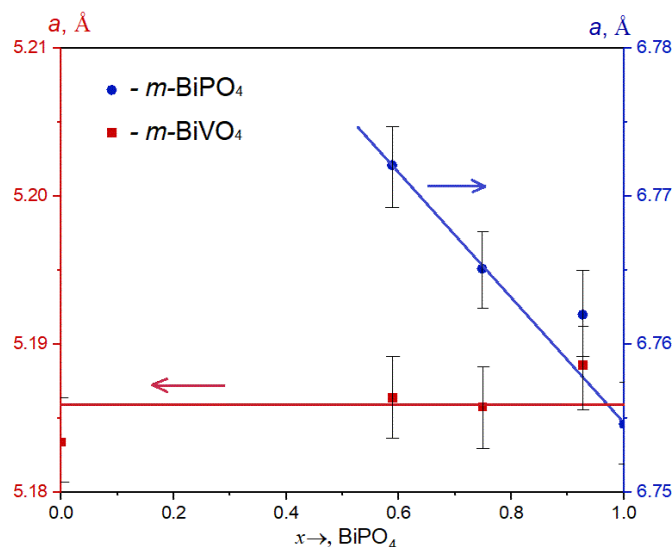


FIG. 2. Dependence of the unit cell parameter a of monoclinic bismuth orthophosphate and orthovanadate on the content of bismuth phosphate in the sample (x)

Graphs of the dependence of the average crystallite size of the coexisting phases on the $\text{BiVO}_4 : \text{BiPO}_4$ ratio are shown in Fig. 3.

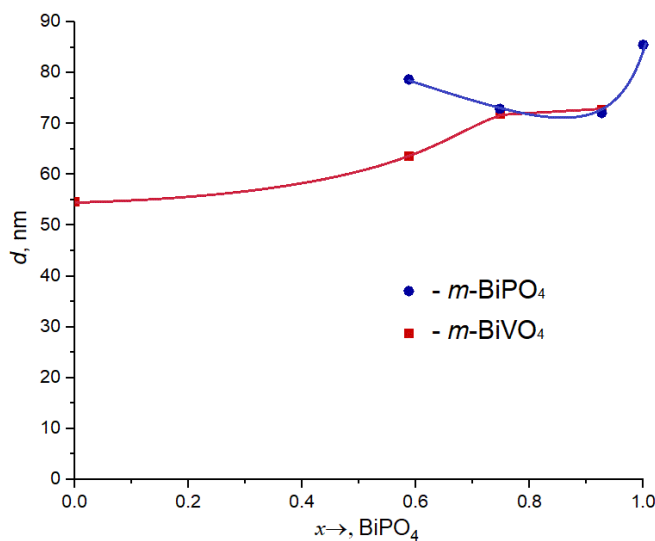


FIG. 3. Dependence of the average crystallite size of the phases of monoclinic bismuth phosphate and bismuth vanadate on the content of bismuth phosphate in the sample (x)

An increase in the amount of bismuth orthophosphate in the system leads to a slight increase in the average size of bismuth orthovanadate crystallites. The size of bismuth orthovanadate crystallites varies within 72 – 85 nm. The crystallites of the $m\text{-BiPO}_4$ phase have the smallest sizes in samples 3 and 4. In addition, in these samples, the average sizes of the crystallites of the $m\text{-BiVO}_4$ phase were closest to the sizes of crystallites of the accompanying $m\text{-BiPO}_4$ phase, and amounted to about 70 nm.

Microphotographs of the samples are shown in Fig. 4. Spot elemental analysis showed that the large particles in the samples are particles of the $m\text{-BiVO}_4$ phase (as an example, a snapshot of sample 3 in Fig. 4c is shown). Smaller particles belong to the $m\text{-BiPO}_4$ phase.

Particle size distributions obtained on the basis of the electron microscopy data are given as an example for sample 4 and are presented in Fig. 5.

On Fig. 6 shows plots of the particle length versus the $\text{BiVO}_4 : \text{BiPO}_4$ ratio in obtained samples.

It can be noted that the particle size of each phase in two-phase samples increases in comparison with single-phase samples with a decrease in the proportion of this phase. Moreover, the average particle length of bismuth orthovanadate increases from 4 to 21 μm with an increasing the proportion of bismuth orthophosphate from 0 to 0.927. Smaller-sized

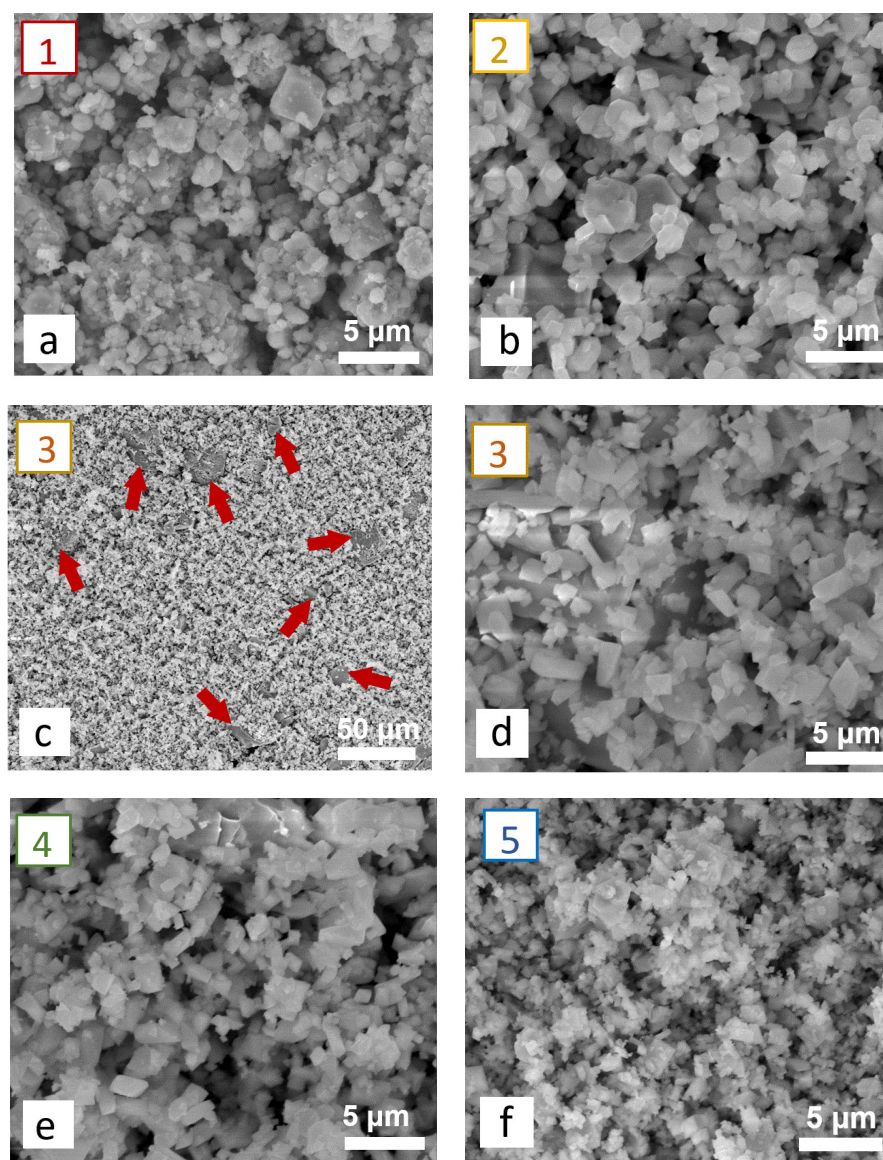


FIG. 4. Micrographs of samples: 1 (a); 2 (b); 3 (c, d); 4 (e), 5 (d) (Arrows point to $m\text{-BiVO}_4$ particles)

particles, have larger the surface area on which photons are absorbed. As a result, there are better photocatalytic properties of substances.

Photocatalytic characteristics of the samples were studied during the decomposition of methyl violet under the action of visible light (Fig. 7). The obtained UV-visible absorption spectra of MV demonstrate the effective destruction of dye molecules over time in the presence of all potential catalysts, as evidenced by the regular decrease in the characteristic peak of MV observed at 578 nm. From the analysis of the obtained spectra, it can be concluded that pure bismuth orthovanadate exhibits the highest photocatalytic activity (sample 1).

Depending on the amount of the bismuth vanadate phase in the samples, the catalytic ability of the samples changes in the following order: $5 > 4 > 3 > 2 > 1$. It can be affected by the morphology of the particles, the size of the crystallites, and the method of catalyst synthesis, its doping, and other factors.

To study the kinetic characteristics of all samples, kinetic curves were constructed, which are the ratio of the concentrations of the reaction solution to the concentration of the initial solution as a function of time (Fig. 8). The resulting curves show the photocatalytic activity of each sample as the exposure time increases and demonstrate a regular decrease in the relative concentration of the dye.

The rate constant of the catalytic reaction was calculated using the linearization of the graph of the dependence of the kinetic curves in pseudo-first-order logarithmic coordinates of the reaction (Fig. 9) and varies from 0.018 to 0.007 min^{-1} depending on the content of bismuth orthophosphate in the samples (Fig. 10).

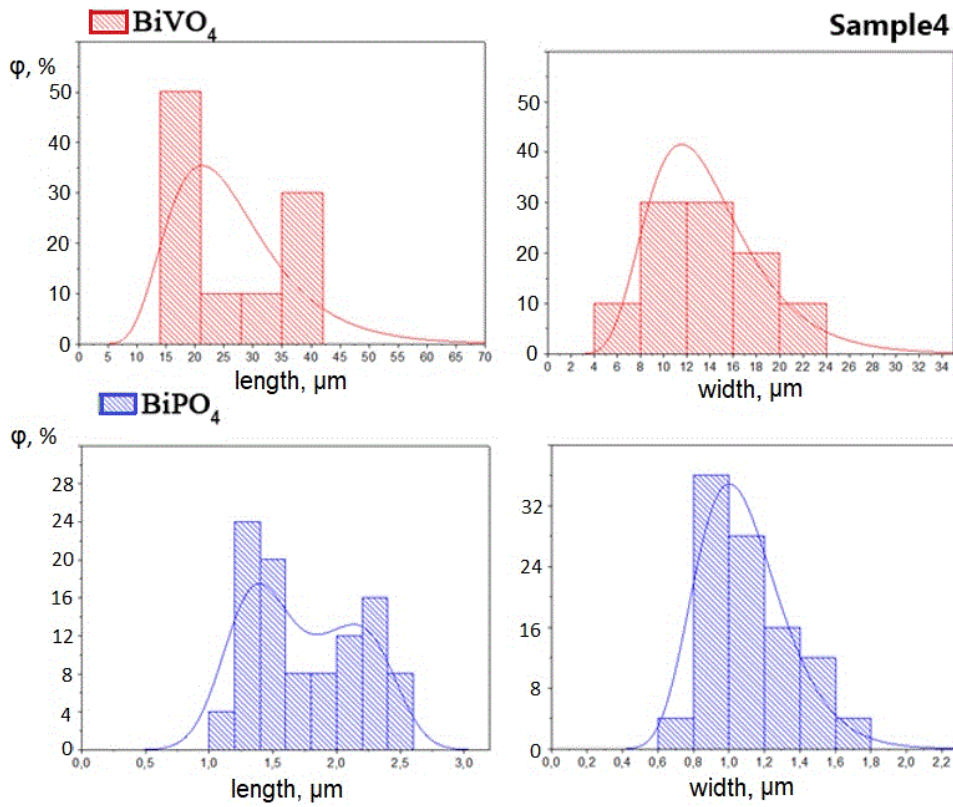


FIG. 5. Particle size distribution in sample 4

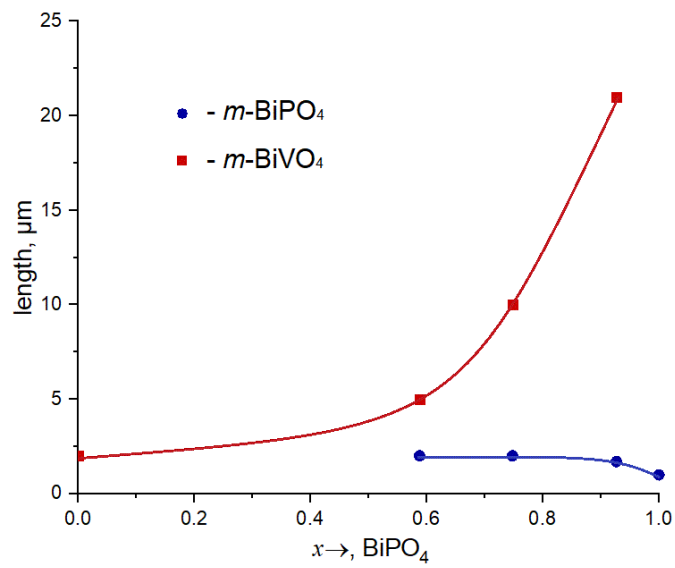
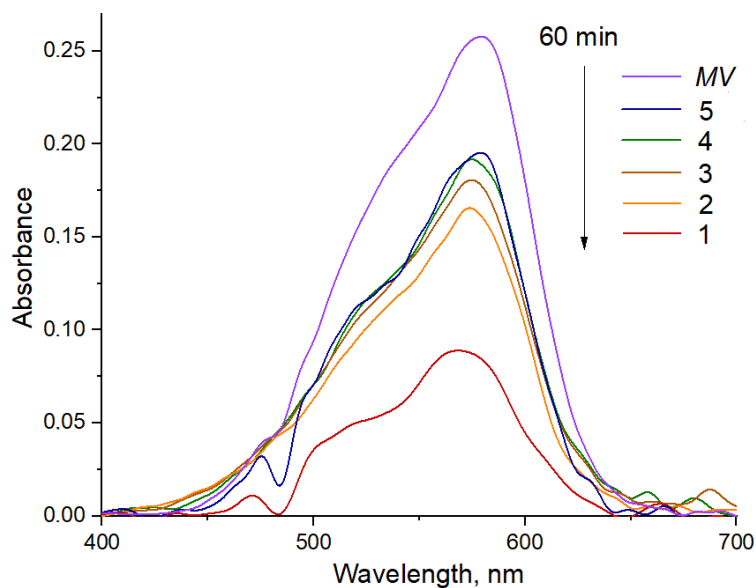
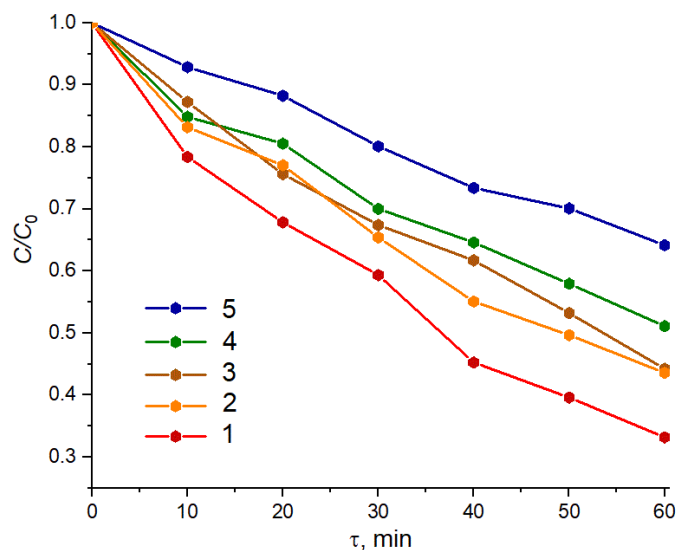


FIG. 6. Graph of average particle length versus bismuth phosphate content in a sample (x)


 FIG. 7. UV-Visible *MV* absorption spectra in the presence of a catalyst under the influence of visible light

 FIG. 8. *MV* degradation profiles of all photocatalysts

4. Conclusion

In the $\text{BiPO}_4\text{-BiVO}_4$ system obtained under hydrothermal conditions (4 hours of isothermal exposure at $200\text{ }^\circ\text{C}$), binary two-phase samples were obtained, which consist of nanocrystalline monoclinic modifications of bismuth vanadate and bismuth phosphate. The bismuth phosphate phase crystallized as a limited solid solution.

It was found that the sizes of crystallites of monoclinic bismuth orthovanadate and the sizes of its particles increased with a decrease in its content in the sample. Sizes of crystallites and particles in the phase based on monoclinic bismuth phosphate BiPO_4 are practically independent of the ratio of coexisting phases in the system.

The photocatalytic activity of obtained nanocrystalline powders in the $\text{BiPO}_4\text{-BiVO}_4$ system was studied during the oxidation of methyl violet. The sample of single-phase bismuth orthovanadate demonstrates a higher catalytic activity. Obtained results can be considered as intermediate for the search of methods for synthesis promising photocatalysts for the oxidation of organic water pollutants.

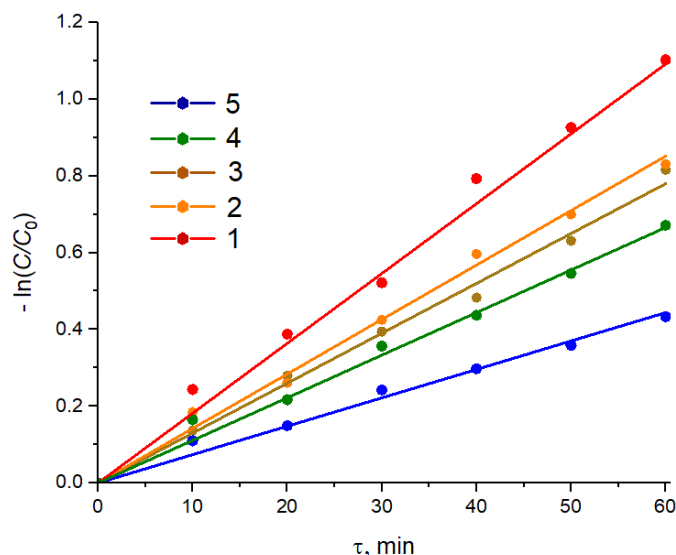


FIG. 9. Kinetic profiles (C/C_0) in logarithmic coordinates for all samples

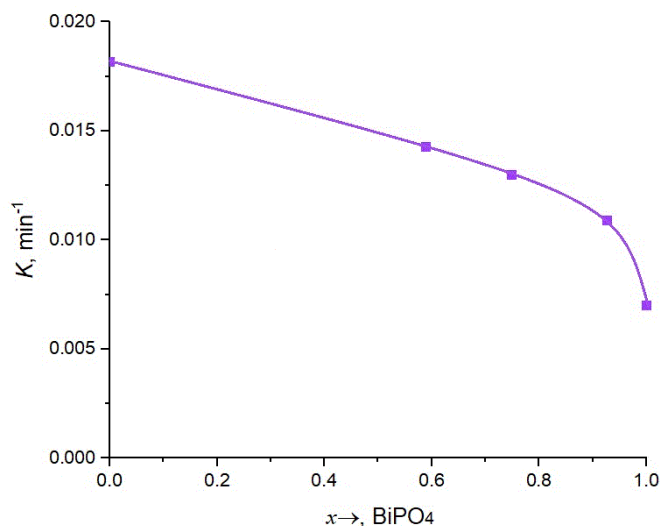


FIG. 10. Dependence of the rate constant of the catalytic reaction on the content of bismuth phosphate in the sample (x)

References

- [1] Malathi A., Madhavan J., Muthupandian Ashokkumar, Prabhakarn Arunachalam. A review on BiVO_4 photocatalyst: Activity enhancement methods for solar photocatalytic applications. *Applied Catalysis A: General*, 2018, **555**, P. 47–74.
- [2] Lin Y.-Y., Chi H.-T., Lin J.-H., Chen F.-H., Chen C.-C., Lu C.-S. Eight crystalline phases of bismuth vanadate by controllable hydrothermal synthesis exhibiting visible-light-driven photocatalytic activity. *Molecular Catalysis*, 2021, **506**, 111547.
- [3] Abdullah A.H., Ali N.M., Tahir M.I.M. Synthesis of bismuth vanadate as visible-light photocatalyst. *Malaysian J. of Analytical Sciences*, 2009, **13** (2), P. 151–157.
- [4] Dolić S.D., Jovanović D.J., Smits K., Babić B., Marinović-Cincović M., Porobić S., Dramićanin M.D. A comparative study of photocatalytically active nanocrystalline tetragonal zircon-type and monoclinic scheelite-type bismuth vanadate. *Ceramics Int.*, 2018, **44** (15), P. 17953–17961.
- [5] Nguyen T.D., Hong S.S. Facile solvothermal synthesis of monoclinic-tetragonal heterostructured BiVO_4 for photodegradation of rhodamine B. *Catalysis Communications*, 2020, **136**, 105920.
- [6] Abdi F.F., Savenije T.J., May M.M., Dam B., van de Krol R. The origin of slow carrier transport in BiVO_4 thin film photoanodes: a time-resolved microwave conductivity study. *The J. of Physical Chemistry Letters*, 2013, **4** (16), P. 2752–2829.
- [7] Jo W. J., Jang J.-W., Kong K., Kang H. J., Kim J. Y., Jun H., Parmar K.P.S., Lee J. S. Phosphate doping into monoclinic BiVO_4 for enhanced photoelectrochemical water oxidation activity. *Angewandte Chemie*, 2012, **124** (13), P. 3201–3205.
- [8] Ganguli S., Hazra C., Chatti M., Samanta T., Mahalingam V. A highly efficient UV–Vis–NIR active Ln^{3+} -doped $\text{BiPO}_4/\text{BiVO}_4$ nanocomposite for photocatalysis application. *Langmuir*, 2016, **32** (1), P. 247–253.
- [9] Shi L., Xue J., Xiao W., Wang P., Long M., Bi Q. Efficient degradation of VOCs using semi-coke activated carbon loaded ternary Z-scheme heterojunction photocatalyst $\text{BiVO}_4\text{-BiPO}_4\text{-}g\text{-C}_3\text{N}_4$ under visible light irradiation. *Physical Chemistry Chemical Physics*, 2022, **24** (37), P. 22987–22997.

- [10] Yang L., Peng S., Yu L., Zhao M. Microstructural, crystallographic, and luminescent analysis after grinding high-temperature monoclinic bismuth phosphate. *J. of Luminescence*, 2020, **225**, P. 117345.
- [11] Zhu Y., Ling Q., Liu Y., Wang H., Zhu Y. Photocatalytic performance of BiPO₄ nanorods adjusted via defects. *Applied Catalysis B: Environmental*, 2016, **187**, P. 204–211.
- [12] Naciri Y., Hsini A., Ajmal Z., Navío J.A., Bakiz B., Albourine A., Ezahri M., Benhachemi A. Recent progress on the enhancement of photocatalytic properties of BiPO₄ using p-conjugated materials. *Advances in Colloid and Interface Science*, 2020, **280**, 102160.
- [13] Buyanova E.S., Emelyanova Yu.V., Morozova M.V., Mikhailovskaya Z.A., Kaymieva O.S., Zhukovskiy V.M., Petrova S.A. Crystal structure and conductivity of bismuth-containing complex oxides. *Chimica Techno Acta*, 2015, **2** (4), P. 306–315.
- [14] Strobel R., Metz H.J., Pratsinis S.E. Brilliant yellow, transparent pure, and SiO₂-coated BiVO₄ nanoparticles made in flames. *Chemistry of Materials*, 2008, **20** (20), P. 6346–6351.
- [15] Gotić M., Musić S., Ivanda M., Šoufek M., Popović S. Synthesis and characterisation of bismuth (III) vanadate. *J. of Molecular Structure*, 2005, **744–747**, P. 535–540.
- [16] Jiang H.-q., Endo H., Natori H., Nagai M., Kobayashi K. Fabrication and photoactivities of spherical-shaped BiVO₄ photocatalysts through solution combustion synthesis method. *J. of the European Ceramic Society*, 2008, **28** (15), P. 2955–2962.
- [17] Manjunatha A.S., Pavithra N.S., Marappa S., Prashanth S.A., Nagaraju G., Puttaswamy Green synthesis of flower-like BiVO₄ nanoparticles by solution combustion method using lemon (Citrus Limon) juice as a fuel: Photocatalytic and electrochemical study. *Chemistry Select*, 2018, **3** (47), P. 13456–13463.
- [18] Kudo A., Omori K., Kato H. A novel aqueous process for preparation of crystal form-controlled and highly crystalline BiVO₄ powder from layered vanadates at room temperature and its photocatalytic and photophysical properties. *J. of the American Chemical Society*. 1999, **121** (49), P. 11459–11467.
- [19] Neves M.C., Trindade T. Chemical bath deposition of BiVO₄. *Thin solid films*, 2002, **406** (1–2), P. 93–97.
- [20] Packiaraj R., Devendran P., Bahadur S.A., Nallamuthu N. Structural and electrochemical studies of Scheelite type BiVO₄ nanoparticles: synthesis by simple hydrothermal method. *J. of Materials Science: Materials in Electronics*, 2018, **29** (15), P. 13265–13276.
- [21] Lin H., Ye H., Chen S., Chen Y. One-pot hydrothermal synthesis of BiPO₄/BiVO₄ with enhanced visible-light photocatalytic activities for methylene blue degradation. *RSC Advances*, 2014, **4** (21), P. 10968–10974.
- [22] Trinh N.D., Hoang H.H., Linh N.X., Vinh N.H., Vu H.T., Nguyen H.T., Vo D.-V.N., Do S.T., Duc L.T. A Facile Synthesis and Properties of Bismuth Vanadate (BiVO₄) Photocatalyst by Hydrothermal Method. *IOP Conference Series: Materials Science and Engineering*, 2019, **542** (1), 012059.
- [23] Zhang A., Zhang J., Cui N., Tie X., An Y., Li L. Effects of pH on hydrothermal synthesis and characterization of visible-light-driven BiVO₄ photocatalyst. *J. of Molecular Catalysis A: Chemical*, 2009, **304** (1–2), P. 28–32.
- [24] Samsudin M.F.R., Sufian S., Bashiri R., Mohamed N.M., Ramli R.M. Synergistic effects of pH and calcination temperature on enhancing photodegradation performance of m-BiVO₄. *J. of the Taiwan Institute of Chemical Engineers*, 2017, **81**, P. 305–315.
- [25] Yan Y., Li X., Ni T., Chang K., Li K., Guo Q. In-situ grafting BiVO₄ nanocrystals on a BiPO₄ surface: Enhanced metronidazole degradation activity under UV and visible light. *J. of the Taiwan Institute of Chemical Engineers*, 2019, **99**, P. 82–92.
- [26] Yan Y., Ni T., Du J., Li L., Fu S., Li K., Zhou J. Green synthesis of balsam pear-shaped BiVO₄/BiPO₄ nanocomposite for degradation of organic dye and antibiotic metronidazole. *Dalton Transactions*, 2018, **47** (17), P. 6089–6101.
- [27] Halder N.C., Wagner C.N.J. Separation of Particle Size and Lattice Strain in Integral Breadth Measurements. *Acta Crystallographica*, 1966, **20** (2), P. 312–313.
- [28] Seroglazova A.S., Popkov V.I. Synthesis of highly active and visible-light-driven PrFeO₃ photocatalyst using solution combustion approach and succinic acid as fuel. *Nanosystems: Phys. Chem. Math.*, 2022, **13** (6), P. 649–654.

Submitted 12 October 2022; revised 12 November 2022; accepted 24 November 2022

Information about the authors:

Olga V. Proskurina – Ioffe Institute, 194021 St. Petersburg, Russia; St. Petersburg State Institute of Technology, 190013, St. Petersburg, Russia; ORCID 0000-0002-2807-375X; proskurinaov@mail.ru

Ilke Diana Chetinel – St. Petersburg State Institute of Technology, 190013, St. Petersburg, Russia; ORCID 0009-0008-7287-298X; diana03ridak@gmail.com

Anna S. Seroglazova – Ioffe Institute, 194021 St. Petersburg, Russia; St. Petersburg State Institute of Technology, 190013, St. Petersburg, Russia; ORCID 0000-0002-3304-9068; annaseroglazova@yandex.ru

Victor V. Gusarov – Ioffe Institute, Politekhnikeskaya St. 26, St. Petersburg, 194021, Russia; ORCID 0000-0003-4375-6388; victor.v.gusarov@gmail.com

Conflict of interest: the authors declare no conflict of interest.